

## Preparation and Characterization of CuWO<sub>4</sub> Nanoparticles

M. A. Ahmed<sup>1</sup>, M. H. Khalil<sup>2</sup>, H. A. El-G hany<sup>3</sup>, and S. A. El-Gharbawy\*<sup>2</sup>

1. Physics Dep., Faculty of Science, Cairo Univ., Giza, Egypt.

2. Housing and Building National Research Center, Giza, Egypt.

3. Physics Dep., Faculty of women for arts, science, and education, Ain Shams Univ.

### Abstract:

In this research work, CuWO<sub>4</sub> nanocomposite powder was prepared via co-precipitation method. The resulting precipitates were annealed at 400°C with heating/cooling rate of 1°C/min. The obtained nanopowder was characterized by X – ray diffraction (XRD), Fourier transformation infrared (FTIR), Environmental Scanning Electron Microscope (ESEM) and High resolution transmission electron microscope (HRTEM). The thermal stability was investigated via differential thermal analysis (DTA) and thermo-gravimetric analysis (TGA). Dielectric constant ( $\epsilon'$ ) and ac electrical conductivity ( $\sigma_{ac}$ ) for the prepared sample were measured in a wide temperature range as a function of frequency.

**Keywords:** Tungsten–Copper, Co-precipitation method, Crystallite size, HRTEM, Electrical properties.

### 1. Introduction:

The W-Cu compound combines the properties of both metals, resulting in a material that is relatively hard, heat-resistant, high-density and self-cooling. It also exhibits superior physical properties at elevated temperatures with High thermal conductivity, and Low thermal expansion together with high arc resistance combined with good electrical conductivity, very high burn-off resistance, high contour sharpness and good machinability. Moreover, W – Cu is able to absorb  $\gamma$  – rays: its ability is larger than that of lead by 30 – 40 %.

Da Costa F. A., et al., (2003) reported on the influence of dispersion technique on the characteristics of W–Cu powders and on its sintering behavior. As stated in their work, using high-energy milling to produce particles containing very fine tungsten grains embedded in copper, called composite particles. A powder consisting of composite particles has an optimal copper dispersion and a very fine tungsten phase. They also obtained a homogeneous fine structure. Kim J. C., Moon I. H., (1998) reported that they have worked on the preparation of W–Cu nanocomposite powder by hydrogen-reduction of ball-milled W and CuO powder mixture. Also, the properties of W–Cu homogeneous nanocomposite produced by thermo-chemical methods were studied [Cheng J., et al., (2006); Ardestani M., et al., (2009)].

In recent years, copper tungstate has attracted increasing interest from the research community because of its numerous possible applications. With a band gap of approximately 2.0–2.3 eV in thin-film form, CuWO<sub>4</sub> has been suggested as a photoanode material candidate for photovoltaic electrochemical (PVEC) cells [Kuzmin K., et al., (2013); Pandey P. K., et al. (2005); Chang Y., et al., (2011)]. The all-solid-state thin-film lithium batteries, which are based on the nanosized CuWO<sub>4</sub> positive electrode proposed by [Kuzmin K., et al., (2013); Li C. L., Fu Z. W., (2008)], show a high-volume rate capacity in the first discharge and lack the unfavorable electrochemical degradation that is observed in liquid electrolyte systems.

Upon being exposed to daylight, the non-crystalline CuWO<sub>4</sub> has been found to have a significantly higher photocatalytic activity than the reference TiO<sub>2</sub> (Degussa P25) when methylene blue undergoes photocatalytic degradation in neutral water [Kuzmin K., et al., (2013); Schmitt P., (2011)]. This result was explained by the intense light absorption in the blue and yellow–red spectral ranges caused by the electronic structure of copper tungstate. A small indirect band gap (2.25 eV [Chang Y., et al., (2011)], 2.3 eV [Ruiz-Fuertes J., et al.,

---

\*Corresponding author | Email : [fouads5649@gmail.com](mailto:fouads5649@gmail.com)

(2008)) and a high stability against photodegradation in water [Yourey J. E., Bartlett B. M.,(2011)] make the mesoporous polycrystalline CuWO<sub>4</sub> thin film a promising candidate for an efficient water-splitting photocatalyst. A structural phase transition to a monoclinic wolframite-type structure was found at 10 GPa[Ruiz-Fuertes J., et al., (2010)], which caused a quenching of the first order Jahn Teller (FOJT) distortion in the CuO<sub>6</sub>octahedra.

The aim of this research is to prepare CuWO<sub>4</sub> nanocomposite by co-precipitation method and to examine its microstructure to recommend its use in the improvement of cementation mortar properties. The prepared samples are easier in preparation, non toxic and environmentally friend.

## 2. Materials and Methods:

CuWO<sub>4</sub> nanocomposite powder was synthesized using co-precipitation method. (Na<sub>2</sub>WO<sub>4</sub>·2H<sub>2</sub>O, >99.0% purity with molecular weight 329.86, LobaChemie, India) and blue colored copper nitrate (Cu(NO<sub>3</sub>)<sub>2</sub>·3H<sub>2</sub>O, >98% purity with molecular weight 241.60, LobaChemie, India) were used as raw materials for synthesis of the composite. The nitrates were weighed in stoichiometric ratios and dissolved separately in triply distilled water. The two solutions were good mixed and droplets of ammonia were added to adjust the pH value to 13. The mixed solution was stirred on a heater up to 90°C for 5 h until bluish green precipitates appear. The precipitate was thoroughly washed and then dried at 150°C. The precipitates were annealed at 400°C for 3 h in Lenton Furnace (UAF 16/5) with heating/cooling rate 1°C/min. XRD was carried out for both as prepared and annealed powder using X-ray diffractometer Phillips model PW / 1710 with Ni filter and CuK $\alpha$  radiation of wavelength 1.542 Å. The X-ray type was operated at 40 kV and 30 mA. FTIR was carried out for this specimen using FT/IR-6300 A using CsI media over a range from 50 to 650 cm<sup>-1</sup> and Jasco FT/IR-6 100 A using KBr media over a range from 400 to 4000 cm<sup>-1</sup>). SEM and EDAX were carried out using Inspect S SEM instrument, HRTEM was carried out using FEI philipsTecnai G<sub>2</sub>S – Twin operated at 200 keV. DTG were carried out using DTG – 60 H Shimadzu. The electrical properties were carried out using the LCR meter (Hioki model 3532 Japan). The dielectric constant ( $\epsilon'$ ) and ac conductivity ( $\sigma_{ac}$ ) of the samples were calculated as a function of absolute temperature at different frequencies ranging from 200 kHz to 4 MHz. For electrical measurements, the powder was pressed using uniaxial pressure of 5x10<sup>8</sup> N/m<sup>2</sup> and then coated using silver paste on the two surfaces. Ohmic contact was also checked for good conductivity.

## 3. Results and Discussion:

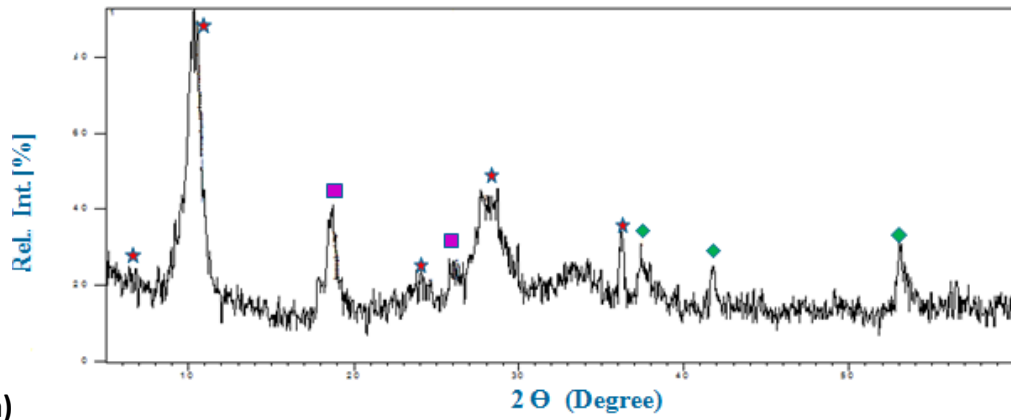
### 3.1. X-ray diffraction (XRD):

X-ray diffraction pattern of as prepared sample is shown in Fig. (1a). The diffraction pattern of it reveals that many phases are present which means that the sample wasn't formed in single phase. After annealing at (400°C), we compared and indexed the diffraction pattern in Fig. (1: b, c) with ICDD card no. (88 – 0269). The phase identification assures the single phase formation in triclinic structure with space group P $\bar{1}$ (2). No extra peaks were observed and all observed lines are broad which indicates that the sample is in nanoscale.

To calculate the crystallite size of copper tungstate nanopowder, Scherrer's formula was used and their findings are reported in table (1). The crystallite size (D) of the powder was calculated by Scherrer's formula, attributing to the entire line broadening to the particle size.

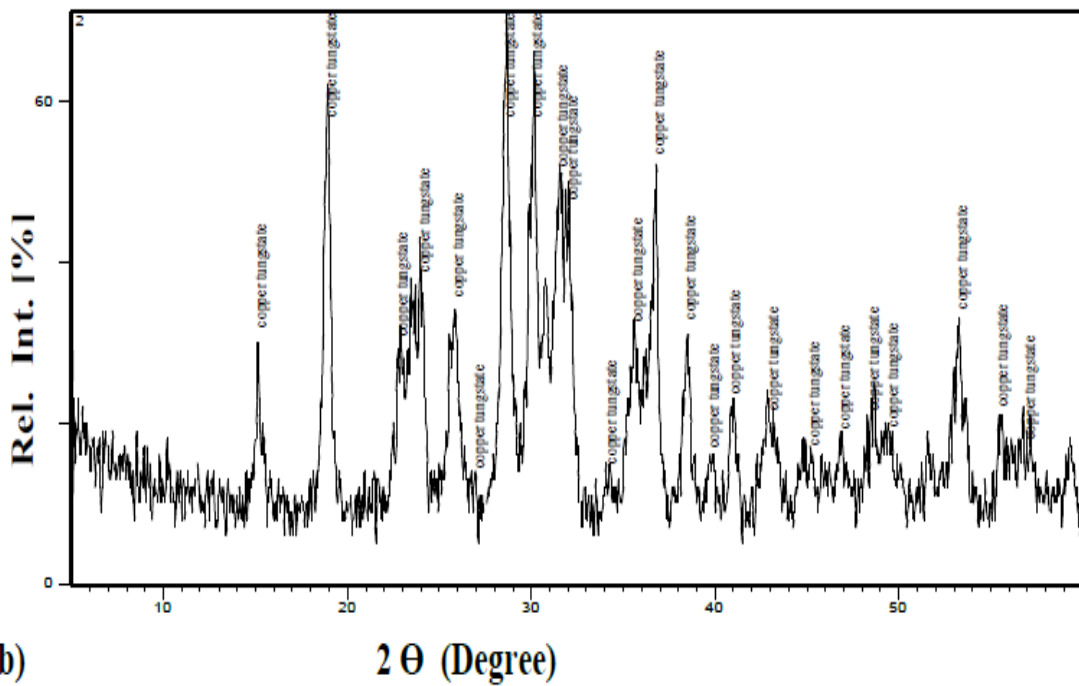
$$D = K\lambda / \beta \cos(\Theta)$$

where, D is crystallite size,  $\beta$  is full width at half maximum of diffraction line in radians,  $\lambda$  is X-ray target wavelength, K is shape factor  $\approx 0.94$ ,  $\Theta$  is diffraction angle for diffraction line.

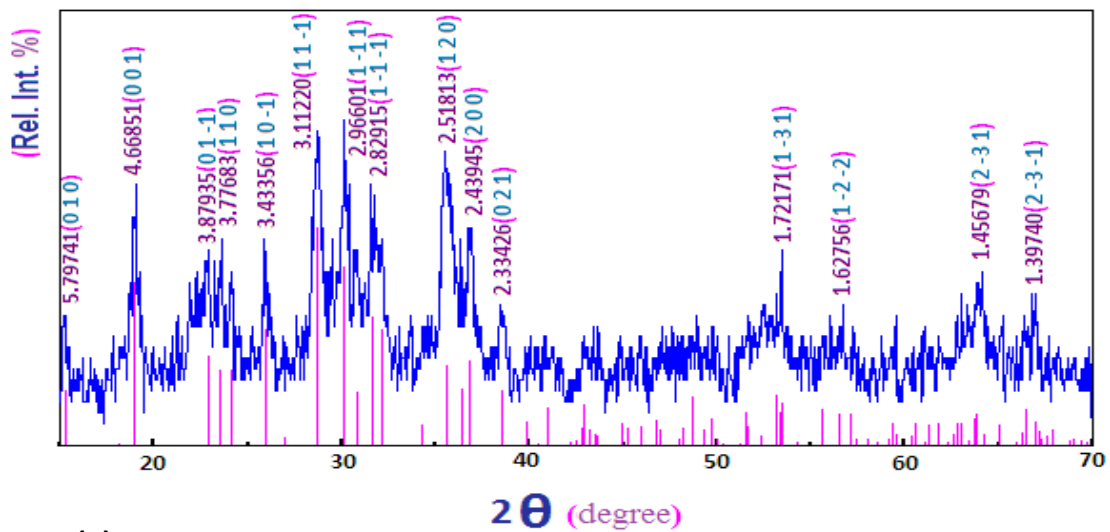


- (a)
- ★ ammonium aquasodium tungstophosphate hydrate
  - ◆ tungsten (IV) oxide
  - tungsten (IV) oxide; ammonium aquasodium tungstophosphate hydrate

Fig. (1a): XRD patterns of the as prepared sample.



(b)



(c)

Fig. (1b, 1c): XRD pattern of the annealed  $\text{CuWO}_4$  sample.

CuWO<sub>4</sub> belongs to a series of structurally related compounds where the transition metal ion plays an important role in structure determination as well as the physico – chemical properties. In these compounds MWO<sub>4</sub>, (M= Mn, Fe, Ni, Co, Cu, Zn, Cd and Mg), the metal cation and tungsten ion occupy non – equivalent octahedral states. CuWO<sub>4</sub> reveals a triclinic crystal structure with space group P $\bar{1}$ (2) unlike the other metal tungstates that adopt wolframite type structure [Kuzmin K., et al., (2013)]. In the former structure (triclinic, P $\bar{1}$ (2)), the metal oxygen Jahn – Teller distorted <CuO<sub>6</sub>> and <WO<sub>6</sub>> of one type are edge shared octahedra. They form Zig Zag chains along the c – axis. These chains are arranged in alternating layers that are perpendicular to the a – axis. The crystal structure is represented in Fig. (2).

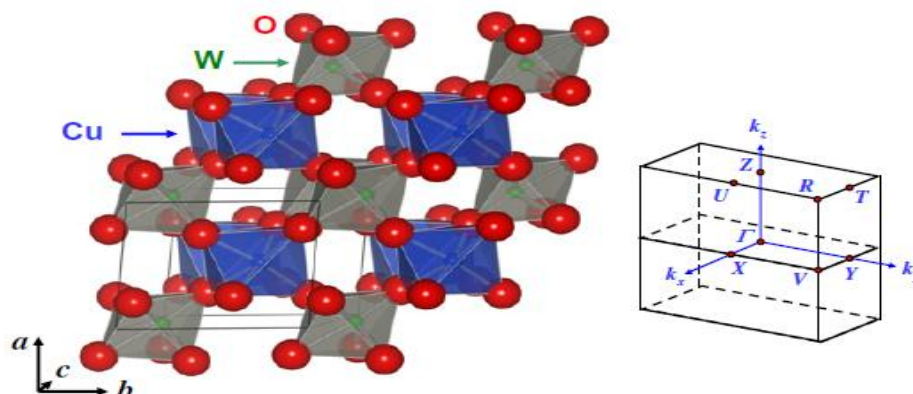


Fig. (2): Crystal structure and first Brillouin zone of triclinic CuWO<sub>4</sub> (space group P $\bar{1}$ (2)).

The <MO<sub>6</sub>> octahedra have different types of distortions. The FOJT distortion results in the axial elongation of the <CuO<sub>6</sub>> octahedra, with the four oxygen in plane atoms are closely located in an approximately square planar configuration and the other two oxygen atoms forms the axial Cu – O bonds. Simultaneously, the other distortion namely second order one (SOJT) results in the out – of – center displacement of tungsten atoms towards the WO<sub>6</sub> octahedra faces. Consequently, this leads to 3 short, 2 intermediate and one long W – O distances [Kuzmin K., et al., (2013)].

Table (1): Values of the d-spacing values; relative intensities and crystallite size as obtained from XRD data of annealed CuWO<sub>4</sub> nanopowder.

Pos. [2 $\theta$ °]	Height [cts]	FWHM [2 $\theta$ °]	d-spacing	Rel. Int. [%]	Cos( $\theta$ ) in radian	Crys. size (nm)
11.6944	8.19	1.8893	7.56739	15.96	0.994802391	<b>4.416948613</b>
12.5429	9.04	1.5744	7.28889	17.96	0.994021572	<b>5.304557985</b>
22.2094	27.4	1.8993	4.00274	53.4	0.981295787	<b>4.454167952</b>
27.5741	8.01	2.2042	3.94869	33.81	0.971217233	<b>3.877865249</b>
28.6893	15.54	2.2542	3.91966	31.84	0.968854391	<b>3.80109859</b>
29.0231	28.36	1.2595	3.07667	55.27	0.968129313	<b>6.808141127</b>
35.2594	51.31	0.8723	2.54549	100	0.953081034	<b>9.985375283</b>
45.3678	5.2	1.2595	2.23437	10.65	0.922723876	<b>7.143156437</b>
48.2289	3.11	0.7446	1.92455	6.17	0.91281832	<b>12.21385366</b>
51.5243	11.66	1.9893	1.74231	23.89	0.900705142	<b>4.633158601</b>
52.5973	9.37	2.152	1.73863	18.26	0.89659994	<b>4.302482566</b>
67.4608	6.56	1.132	1.40564	13.43	0.831825303	<b>8.816202111</b>
<b>The Average Crystallite side is <math>\approx</math> 6nm</b>						<b>6.0855278</b>

The average crystallite size as calculated from XRD was found to be 6nm which is considered very small and is reported for the first time at very low annealing temperature.

### 3. 2. Thermal study (DTA, TGA):

Figure (3) illustrates the differential thermogravimetry (DTA/TGA) thermograph for the  $\text{CuWO}_4$  annealed nanopowder. From the TGA plot it is evident that there is no significant weightloss from room temperature up to about ( $894^\circ\text{C}$ ). The first and second steps in the weightloss are observed at ( $894^\circ\text{C}$ ) and at ( $946^\circ\text{C}$ ). The observed weightloss could be regarded as minimum and didn't exceed 2.0% at such high temperatures; these results assure the high thermal stability of the nanopowder under investigation. Moreover, this result recommended the use of such compounds in nanoform in high temperature applications.

In DTA thermograph, a large plateau was found at ( $200^\circ\text{C} \leq T \leq 800^\circ\text{C}$ ). After that, two endothermic peaks appeared the first at ( $810^\circ\text{C}$ ) and the second at ( $844^\circ\text{C}$ ). The later could be related to a structural phase transformation. These phase transformations might be attributed to first and second order Jahn – Teller distortion of  $\langle\text{CuO}_6\rangle$  and  $\langle\text{WO}_6\rangle$  octahedra.

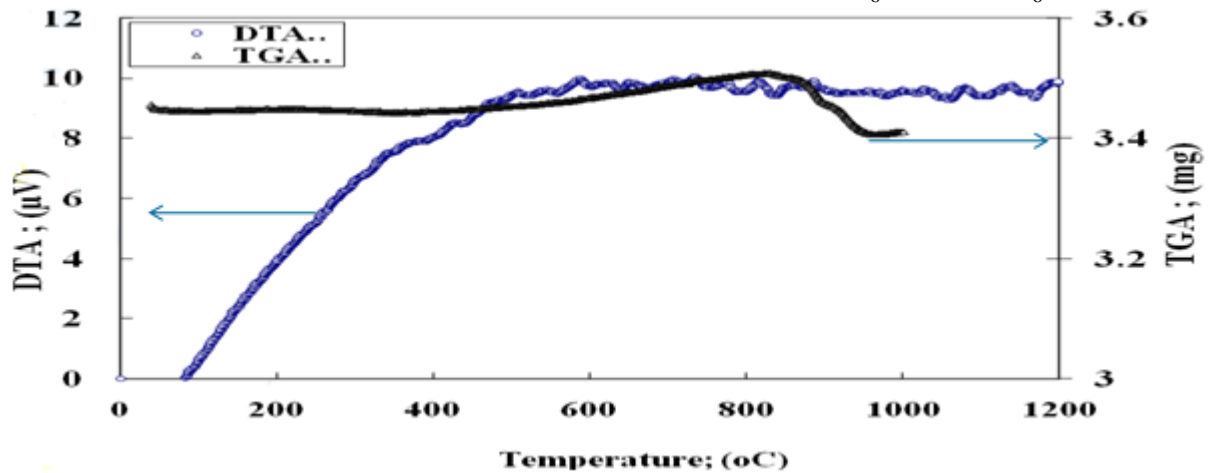


Fig. (3): illustrates the plots of DTA and TGA of the  $\text{CuWO}_4$  sample after annealing at  $400^\circ\text{C}$ .

### 3. 3. The environmental scanning electron microscope (ESEM):

Figure (4) illustrates the environmental scanning electron micrography of the annealed sample  $\text{CuWO}_4$  at two different magnifications. The micrograph (a) reveals homogeneous distribution of the grains. At higher magnification (b) the grains appear to have Cauliflower shape of small size and homogeneous distribution. The grains are arranged in a network of concentric like spheres. The ultrafine size of the particulates is the main reason of the appeared agglomeration in some regions. Energy dispersive X-ray(EDAX) data is represented in Fig.(5) and table (2) and the nominal ratio of Cu/W was found to be W–30wt% Cu.

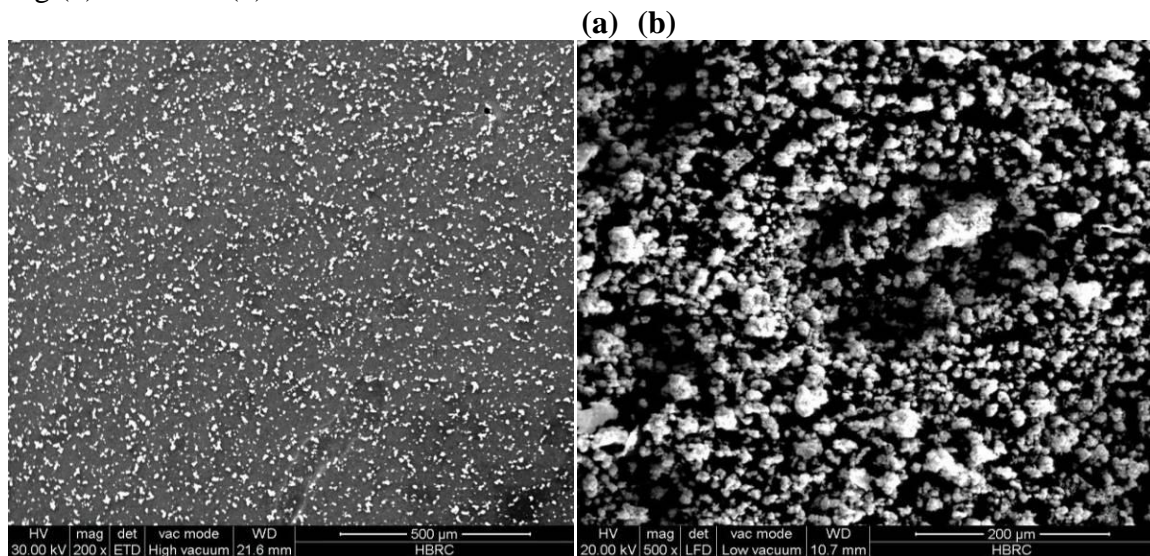


Fig. (4): SEM of the annealed  $\text{CuWO}_4$  sample. (a) The Fig. with magnification 200, (b) The Fig. with magnification 500.



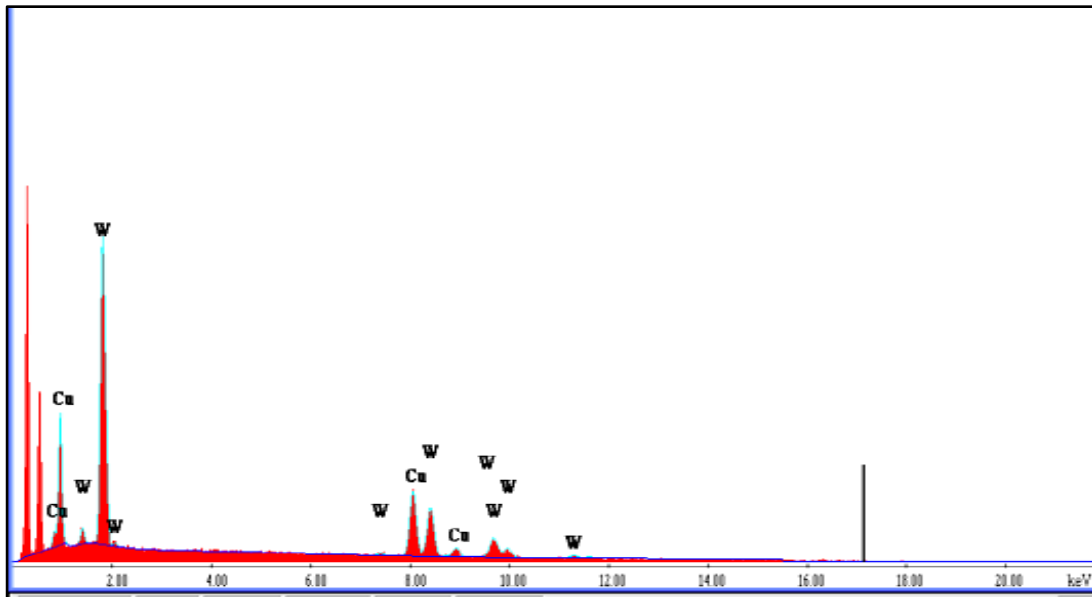


Fig. (5): The EDAX of the annealed  $\text{CuWO}_4$  sample.

Table (2): The EDAX values of the annealed  $\text{CuWO}_4$  sample.

Element	Wt %	At %	K – Ratio
Cu K	29.92	55.27	0.3308
W L	70.08	44.73	0.6553
Total	100.0	100.0	1.0

### 3. 4.High resolution transmission electron microscope (HRTEM):

Figure (6) illustrates the high resolution transmission electron micrograph for  $\text{CuWO}_4$  nanoparticles. The micrograph reveals rod like shape particles with relatively large aspect ratio, the average rod length is 60 nm and its diameter didn't exceed 10 nm. These particles are arranged in an elongated manner attached to each other in a preferred orientation.

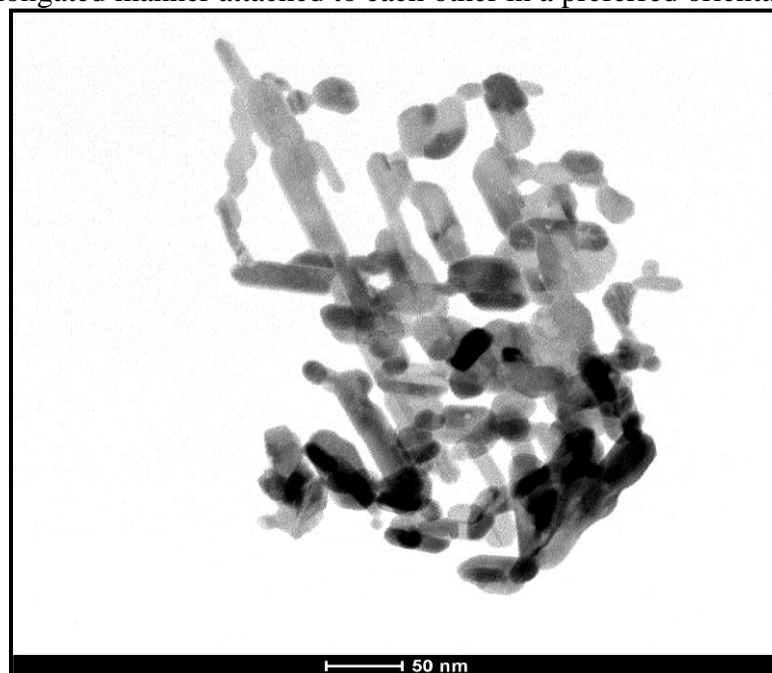


Fig. (6): HRTEM of the annealed  $\text{CuWO}_4$  sample.

### 3. 5. Electrical properties:

Figure (7a) correlates the dielectric constant ( $\epsilon'$ ) with absolute temperature at different frequencies. The data reveals initial little decrease of ( $\epsilon'$ ) at 300 °K. Then it remains constant and a stable trend starts to predominate up to about 540 °K. After that, ( $\epsilon'$ ) increased with a larger rate up to a large hump centered at about 600 °K. At  $T \geq 650$  °K data reveals very rapid increasing. Fig. (7b) shows that the ac conductivity ( $\sigma_{ac}$ ) reveals nearly the same trend of ( $\epsilon'$ ) because polarization and conductivity are of the same origin.

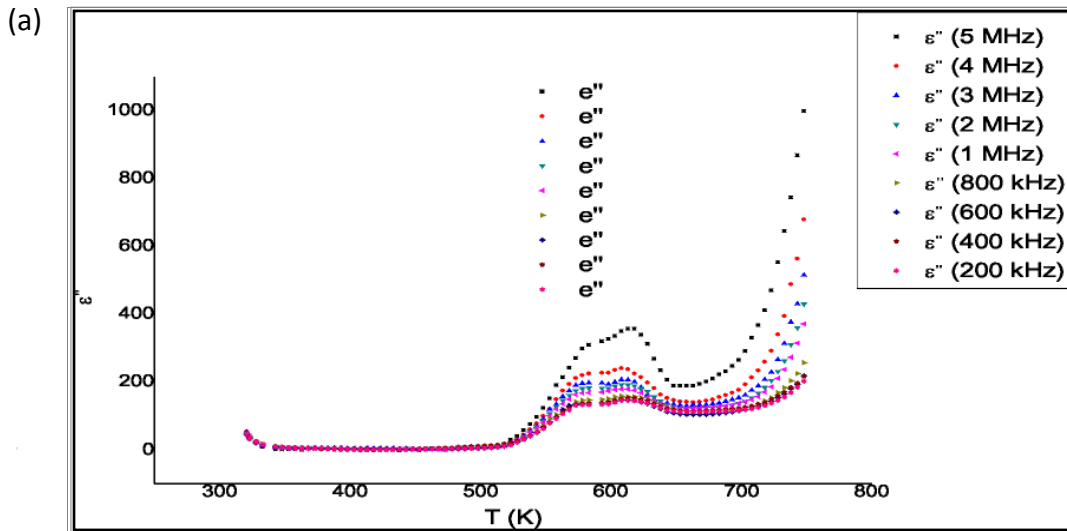


Figure (7 a): Correlates the variation of the real part of the dielectric constant ( $\epsilon'$ ) with absolute temperature for the annealed  $\text{CuWO}_4$  sample at different frequencies.

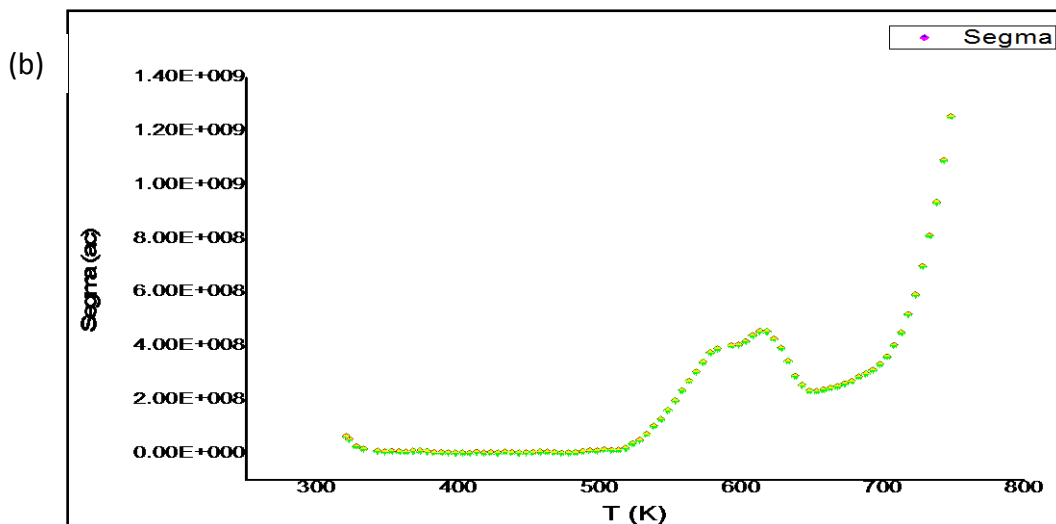


Figure (7b): Shows the variation of the ac conductivity with absolute temperature for the annealed  $\text{CuWO}_4$  sample at different frequencies.

### 3. 6. Fourier transformation infrared (FTIR):

The FTIR spectra of the prepared  $\text{CuWO}_4$  nanopowder are illustrated in Fig. (8). Figs. (8a, 8c) reveal the appearance of different transmittance bands. Fig. (8b) reveals the appearance of different absorbance bands. The band position and their assignments are reported in table (3).

Table (3): FTIR of the annealed CuWO<sub>4</sub> sample.

$\nu\text{cm}^{-1}$	Bond	assignment	References
469	W – O – W	Deformation bridging mode	[Naik S. J., Salker A. V.,(2010); Zhang H., Xijun H.,(2004)]
550	Cu – O	Stretching vibration	[Olivante L. V., (2008)]
600	O – Cu – O	Anti-symmetric vibration	Olivante L. V., (2008)]
703	W-O-W	$\gamma$ (W-O-W)	[Pfeifer J., et al., (1995); Díaz-Reyes J., et al., (2008)]
790	Cu – O	stretching	[Naik S. J., Salker A. V.,(2010)]
910	Cu <sup>n+</sup> – O <sup>2-</sup> – W <sup>n+</sup>	vibration	[Damia n M. A., et al., (2003); Clark G. M., Doyle W. P., (1966); Arora S. K., et al., (1988)]
3400	O – H	Stretching vibration	[Olivante L. V., (2008)]

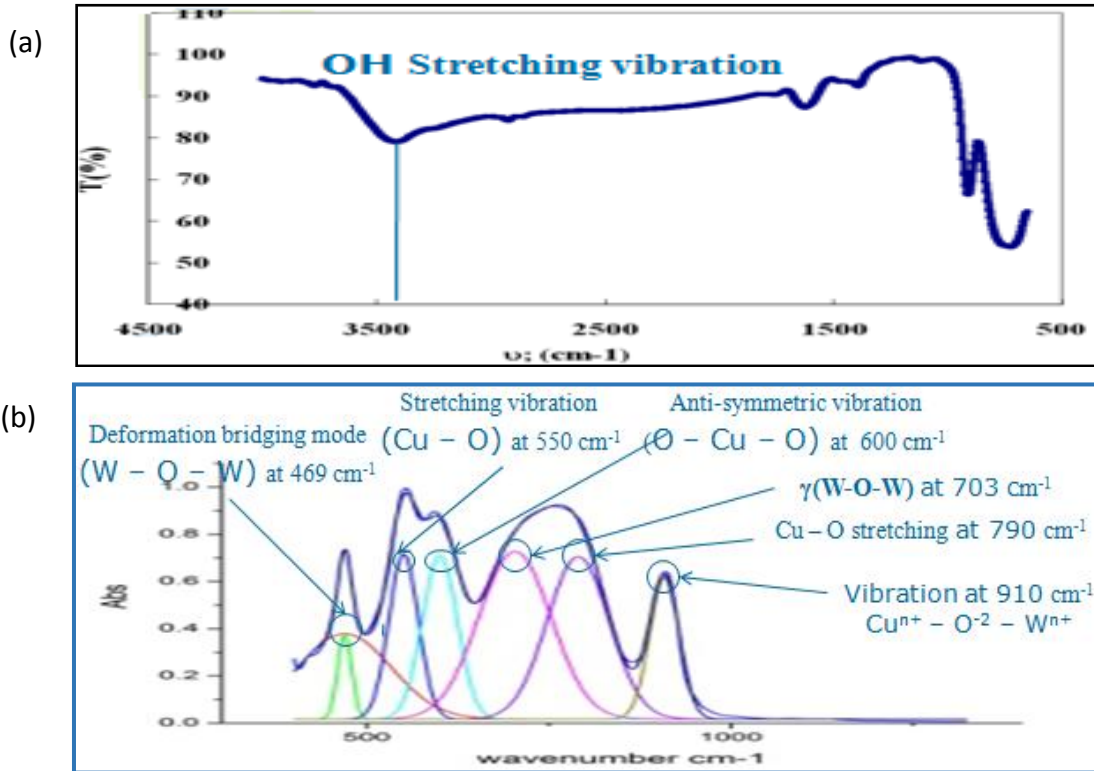


Figure (8a, 8b): FTIR of the annealed CuWO<sub>4</sub> sample in the range (400 – 4000 cm<sup>-1</sup>).

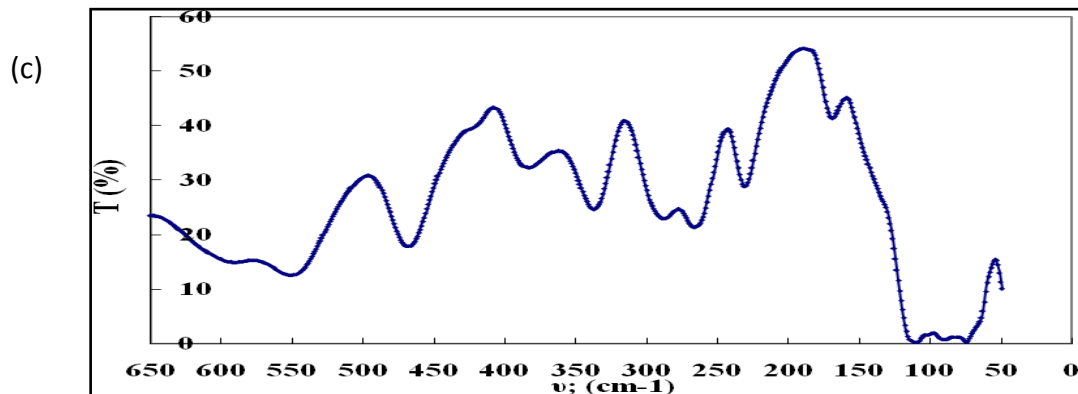


Figure (8c): FTIR of the annealed CuWO<sub>4</sub> sample in the range (50 – 650 cm<sup>-1</sup>).



#### 4. Conclusion:

**The results of this study were summarized as:**

1. The phase identification assures the single phase formation in triclinic structure with space group  $P\bar{1}(2)$ .
2. The average crystallite size as calculated from XRD was found to be 6nm which is considered very small and is reported for the first time at very low annealing temperature.
3. DTA/TGA thermograph for the  $\text{CuWO}_4$  annealed nanopowder show no significant weightloss from room temperature up to about (810°C).
4. The first and second steps in the weightloss are observed at (810°C) and at (894°C).
5. The weightloss could be regarded as minimum and didn't exceed 2% at such high temperatures
6. These results assure the high thermal stability of the nanopowder under investigation, which recommended the use of such compounds in nanof orm in high temperature applications.
7. The DTA thermograph clears a large plateau at ( $200^\circ\text{C} \leq T \leq 800^\circ\text{C}$ ). Two endothermic peaks appear the first at (844°C) and the second at (946°C). The later could be related to a structural phase transformation. These phase transformations might be attributed to first and second order Jahn –Teller distortion of  $\langle\text{CuO}_6\rangle$  and  $\langle\text{WO}_6\rangle$  octahedra.
8. The grains of the nanopowder appear to have Cauliflower shape of small size and homogeneous distribution. The grains are arranged in a network of concentric like spheres.
9. The ultrafine size of particulates is the main reason of the appeared agglomeration in some regions. The nominal ratio of Cu/W was found to be W–30% Cu.
10. The high resolution transmission electron micrograph for  $\text{CuWO}_4$  nanoparticles reveals rod like shape particles with relatively large aspect ratio, The average rod length is 60 nm and its diameter didn't exceed 10 nm. These particles are arranged in an elongated manner attached to each other in a preferred orientation.
11. The dielectric constant ( $\epsilon'$ ) with absolute temperature at different frequencies reveals initial little decrease of ( $\epsilon'$ ) at 300 °K. Then it remains constant and a stable trend starts to predominate up to about 540 °K. After that, ( $\epsilon'$ ) increased with a larger rate up to a large hump centered at about 600 °K existed. At  $T \geq 650$  °K data reveals very rapid increasing.
12. The ac conductivity reveals nearly the same trend of  $\epsilon'$  because polarization and conductivity are of the same origin.
13. The FTIR spectrum of the prepared  $\text{CuWO}_4$  nanopowder reveals the appearance of different transmittance bands.

## References:

- Ardestani M., Arabi H., Rezaie H. R., Razavizadeh. H.,** *Int. J. Refract. Met. Hard Mater.*, 27, 796–800 (2009).
- Arora S. K., Mathew T., Batra N. M.,** *J. Cryst. Growth*, 88, 379 (1988).
- Chang Y., Braun A., Deangelis A., Kaneshiro J., Gaillard N.,** *J. Phys. Chem. C*, 115, 25490 (2011).
- Cheng J., Lei C., Xiong E., Jiang Y., Xia Y.,** *J. Alloys Compd.*, 421, 146–150 (2006).
- Clark G. M., Doyle W. P.,** *Spectrochim. Acta*, 22, 1441 (1966).
- Da Costa F. A., Da Silva A. G. P., Gomes U. U.,** *Powder Technology*, 134(1-2), 123–132 (2003).
- Damia n M. A., Rodriguez Y., Solis J. L., Estrada W.,** *Thin Solid Films*, 444, 104–110 (2003).
- Díaz-Reyes J., Dorantes-García V., Pérez-Benítez A., Balderas-López J. A.,** *Superficies y*, 21(2), 12–17 (2008).
- Kim J. C., Moon I. H.,** *Nanostructured Materials*, 10 (2), 283–290 (1998).
- Kuzmin K., Kalinko A., Evarestov R. A.,** *Acta Material*, 61, 371–378 (2013).
- Li C. L., Fu Z. W.,** *Electrochim. Acta*, 53, 4293 (2008).
- Naik S. J., Salker A. V.,** *Solid State Sciences*, 12 (12), 2065–2072 (2010).
- Olivante L. V.,** *Materials science research trends*, Nova Science Publisher, Inc., (2008).
- Pandey P. K., Bhave N. S., Kharat R. B.,** *Mater Lett*, 59, 3149 (2005).
- Pfeifer J., Guifang C., Tekula-Buxbaum P., Kiss B. A., Farkas-Jahnke M., Vadasdi K.,** *J. Solid State Chem.*, 119, 90 (1995).
- Ruiz-Fuertes J., Errandonea D., Lacomba-Perales R., Segura A., Gonzalez J., Rodriguez J., et al.,** *Phys. Rev. B*, 81, 224115 (2010).
- Ruiz-Fuertes J., Errandonea D., Segura A., Manjn F. J., Zhu Z. H., Tu C. Y.,** *High Pressure Res.*, 28, 565 (2008).
- Schmitt P., Brem N., Schunk S., Feldmann C.,** *Adv. Funct. Mater.*, 21, 3037 (2011).
- Yourey J. E., Bartlett B. M.,** *J Mater. Chem.*, 21, 7651 (2011).
- Zhang H., Xijun H.,** *Separ. Purif. Tech.*, 34, 105–108 (2004).

## ملخص البحث باللغة العربية

### "تحضير وتوصيف مادة $CuWO_4$ النانومترية"

محمد علي أحمد<sup>1</sup>، مرفت حسن خليل<sup>2</sup>، هيام أحمد عبد الغني<sup>3</sup>، سحر أحمد فؤاد الغرباوي<sup>2</sup>

1. قسم الفيزياء – كلية العلوم – جامعة القاهرة.
2. معهد طبيعة المنشآت – المركز القومي لبحوث الإسكان والبناء.
3. قسم الفيزياء – كلية البنات للآداب والعلوم والتربية – جامعة عين شمس.

تم في هذا البحث استخدام طريقة الترسيب الكيميائي الحراري "thermo-chemicalco-precipitation" وذلك لتحضير مادة  $CuWO_4$  النانومترية على شكل مسحوق. وقد تم تسخين المادة المترسبة عند درجة حرارة 400 درجة مئوية بمعدل تسخين/تبريد مقداره 1 درجة مئوية في الدقيقة. وقد تم إجراء الاختبارات اللازمة على المادة التي تم الحصول عليها. وقد أثبت اختبار X – ray diffraction (XRD) أن مادة  $CuWO_4$  النانومترية عالية النقاوة وذات حجم بللوري في حدود 6 نانومتر ، كما أثبت اختبار differential thermal analysis (DTA) واختبار Thermogravimetric analysis (TGA) أن تلك المادة ذات ثبات حراري عند درجات الحرارة المرتفعة (810°س). وتم أيضا إجراء اختبار Fourier transformation infrared (FTIR) وذلك لمعرفة أنواع الروابط الكيميائية لهذه المادة. وكذلك تم عمل اختبار Environmental Scanning Electron Microscope (ESEM) وقد أثبت أن المادة متجانسة الشكل فيما عدا بعض التجمعات أو التراكمات التي قد تكون نتيجة أن جزيئات تلك المادة متناهية الصغر. بالإضافة إلى أنه تم إجراء اختبار High resolution transmission electron microscope (HRTEM) وقد أكد نتائج الاختبارات السابقة (XRD) , (ESEM) و أوضحت الصور أن شكل المادة كان عبارة عن قضبان متماسكة بشكل منتظم وطولها لا يزيد عن 60 نانومتر وعرضها لا يزيد عن 10 نانومتر. إضافة إلى ذلك تم قياس الخواص الكهربائية للمادة عند درجات الحرارة المختلفة من 321°كلفن إلى 748°كلفن في مدى واسع من الترددات الكهربائية من 200 كيلو هرتز إلى 5 ميجا هرتز.